1

Simulation of Max-Stable Processes

Marco Oesting

INRA/AgroParisTech

Mathieu Ribatet

Université Montpellier 2

Clément Dombry

Université de Franche-Comté

CONTENTS

Abstract

Simulation of stochastic phenomena has become an important tool to assess characteristics which are analytically intractable. In this chapter, we deal with the problem of sampling from max-stable processes, which, by the spectral representation (de Haan, 1984), require taking the pointwise maxima over an infinite number of spectral functions belonging to a Poisson point process. In

practice, spectral functions are simulated in an appropriate order until some stopping rule takes effect. For mixed moving maxima processes with bounded shape functions with joint compact support, Schlather (2002) provides such a stopping criterion yielding an exact simulation. Oesting et al. (2013) consider stopping rules for a family of equivalent spectral representations in a very general setting, particularly focusing on the normalized spectral representation which allows for an exact simulation, as well. Although this representation exists under mild conditions, the distribution of the corresponding spectral functions might be inappropriate for sampling. In this case, approximative procedures are proposed. Here, the choice of the stopping rule and the spectral representation is crucial for the quality of approximation. In this context, we discuss measures of simulation efficiency and quality. Several examples of max-stable processes are analyzed. We particularly focus on the challenging case of Brown-Resnick processes which are stationary although originally constructed via non-stationary spectral functions. Finally, we review existing `R` packages on the simulation of max-stable processes.

1.1 Introduction

Max-stable processes have become frequently used models for spatial extremes. However, due to their rather sophisticated structure, in many cases, analytical expressions are available for the bivariate (or sometimes also trivariate) distributions of the process only. Thus, in order to assess some more advanced characteristics of the process which are of interest in practical applications, stochastic simulation is used. Further, the problem of simulation of max-stable processes is closely related to the questions of conditional simulation and prediction of max-stable processes given observations at some locations (see Chapter ?? for details).

In the following, we will deal with the problem of simulation of a sample-continuous max-stable process Z on some compact domain $\mathcal{X} \subset \mathbb{R}^d$. Without loss of generality, we may assume that Z has unit Fréchet margins. Realizations of a process with arbitrary generalized extreme value marginal distributions can be obtained by marginal transformations.

Remind that, the process Z allows for a spectral representation (cf. de Haan, 1984; Giné et al., 1990; Penrose, 1992) of the form

$$Z(x) = \max_{i \geq 1} \zeta_i \psi_i(x), \quad x \in \mathcal{X}, \tag{1.1}$$

where $\{(\zeta_i, \psi_i)\}_{i \geq 1}$ is a Poisson point process on $(0, \infty) \times \mathcal{C}$ with intensity measure $\zeta^{-2} \, \mathrm{d}\zeta \times \nu(\mathrm{d}\psi)$ for some locally finite measure ν on the space $\mathcal{C} = C(\mathcal{X}, [0, \infty))$ of continuous non-negative functions on $\mathcal{X}$ such that

$$\int \psi(x) \, \nu(\mathrm{d}\psi) = 1, \quad x \in \mathcal{X}. \tag{1.2}$$

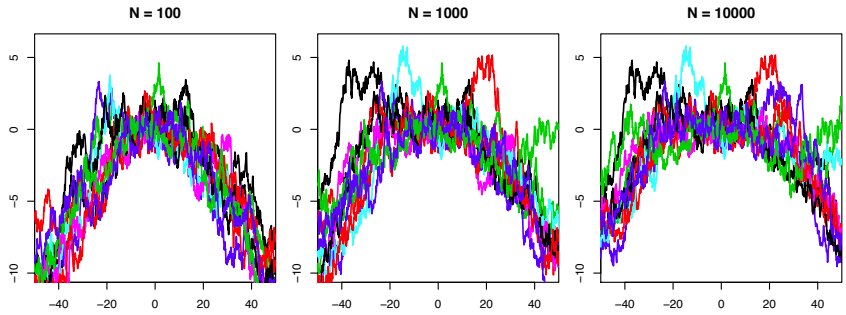

FIGURE 1.1
Ten approximations of $\log Z$ on the interval $[-50, 50]$ by taking the maximum over the first N spectral functions with $N = 100$, 1000, 10000 (from left to right). Here, Z is a Brown-Resnick process associated to the semi-variogram $\gamma(h) = \frac{1}{2}|h|$.

The aim of this chapter is the simulation of the process Z on $\mathcal{X}$. According to representation (1.1), Z is constructed as the pointwise maximum of an infinite number of functions. Thus, exact simulation of Z is in general not straightforward. In many cases, the Poisson points $\{(\zeta_i, \psi_i)\}_{i\geq 1}$ can be subsequently simulated such that $\zeta_{i+1} \leq \zeta_i$ for all $i \geq 1$ (see Section 1.2). This motivates the strategy of approximating Z by the maximum over the "first" N points where the finite number N is given by some stopping criterion.

Although this procedure might be quite efficient in some cases, there are examples where this straightforward approach also encounters severe problems. Such examples contain the important class of Brown-Resnick processes (Kabluchko et al., 2009) where the spectral measure ν in representation (1.1) is the probability measure of the stochastic process $Y(t) = \exp(W(t) - \sigma^2(t)/2)$. Here, $W(\cdot)$ is a centered Gaussian process with stationary increments, semi-variogram γ and variance $\sigma(\cdot)$. Thus, the Brown-Resnick process Z associated to the semi-variogram γ can be written as

$$Z(t) = \max_{i\geq 1} \zeta_i \exp(W_i(t) - \sigma^2(t)/2), \quad t \in \mathbb{R}^d, \tag{1.3}$$

where $\{\zeta_i\}$ are the points of a Poisson point process with intensity $\zeta^{-2}\,\mathrm{d}\zeta$ and W_i, $i \geq 1$, are independent copies of W.

Then, the max-stable process Z is stationary although the spectral process Y is not. Thus, a challenge for an accurate simulation of Z is the visualization of stationarity. However, as Figure 1.1 shows for the example of Brown-Resnick process associated to the semi-variogram $\gamma(h) = \frac{1}{2}|h|$, considered first by Brown and Resnick (1977), finite approximations obtained in the above way may depict clear trends even for a large number N of considered spectral functions. Thus, in this case, a more sophisticated procedure is needed for an accurate approximation. This motivates a careful analysis of different cases.

The chapter is organized as follows: In Section 1.2, we present the basic procedure of simulation. We focus on two important classes of spectral representations — the representation via stochastic processes and the mixed moving maxima representation — and consider subclasses which allow for an exact simulation by Schlather's (2002) algorithm. Section 1.3 deals with transformations that allow to switch between different, but equivalent spectral representations and the according simulation procedures. Here, we place particular emphasis on the so-called normalized spectral representation which enables exact simulation. Further, we provide a measure for efficiency to compare different exact simulation procedures. Due to the complexity of exact simulation, it may be worthwhile to consider approximative algorithms. Error estimates are given in Section 1.4. In Section 1.5, we discuss accurate simulation for several examples including some of the most commonly used classes of max-stable processes. Finally, we present an overview over `R` packages on the simulation of max-stable processes (Section 1.6).

1.2 Basic Procedure and Stopping Rules

In the following, we always assume that Z is a max-stable process on a compact domain $\mathcal{X} \subset \mathbb{R}^d$ with spectral representation (1.1). As this representation just requires the spectral measure ν to be a locally finite measure on $\mathcal{C}$ satisfying condition (1.2), the class of max-stable processes contains a large variety of models potentially requiring different procedures for an accurate simulation. Thus, we first restrict ourselves to two important classes of max-stable processes, namely the class of processes which are represented via stochastic processes (i.e. the spectral measure is a probability measure) and the class of mixed moving maxima processes. In both cases, we consider subclasses that allow for an exact simulation in finite time by algorithms devised by Schlather (2002). In Section 1.3, we will see how transformations of the spectral measure allow us to reduce simulation problems to these cases. Thus, the procedures presented in this section also prove useful in a more general setting.

1.2.1 Representation via Stochastic Processes

First, we consider the case that ν is a probability measure. Then, the corresponding process Z possesses a Penrose (1992)-type representation:

$$Z(x) = \max_{i \geq 1} \zeta_i Y_i(x), \qquad x \in \mathcal{X}, \tag{1.4}$$

where $\{\zeta_i\}_{i \geq 1}$ is a Poisson point process on $(0, \infty)$ with intensity measure $\zeta^{-2} \mathrm{d}\zeta$ and Y_i, $i \geq 1$, are independently distributed according to the probability measure ν. According to condition (1.2), the processes Y_i necessarily satisfy $\mathbb{E}Y_i(x) = 1$ for all $x \in \mathcal{X}$. As the spectral functions Y_i allow

for an interpretation as independent stochastic processes, we call the spectral representation (1.4) a *representation via stochastic processes*. Examples of max-stable processes with such a representation are Brown-Resnick processes (Kabluchko et al., 2009) where Y_i is a log-Gaussian process or extremal t processes (Opitz, 2013) where Y_i is the positive part of a Gaussian process to some positive power α, including the particular case of an extremal Gaussian process (Schlather, 2002) with $\alpha = 1$.

For simulation of the Poisson point process $\{\zeta_i\}_{i\geq 1}$, we note that, by the mapping theorem, $\{\zeta_i^{-1}\}_{i\geq 1}$ is a standard Poisson point process on $(0,\infty)$, i.e. $\zeta_1^{-1}, \zeta_2^{-1} - \zeta_1^{-1}, \zeta_3^{-1} - \zeta_2^{-1}, \ldots$ are independent and standard exponentially distributed. Thus, for Z as defined in (1.4), we obtain the equality

$$Z(x) =_d \max_{i\geq 1} \frac{Y_i(x)}{\sum_{j=1}^i E_j}, \quad x \in \mathcal{X}, \tag{1.5}$$

for $E_j \sim_{iid} \mathrm{Exp}(1)$, $j \geq 1$, where $\mathrm{Exp}(\lambda)$ denotes the exponential distribution with parameter $\lambda > 0$ and $=_d$ denotes equality in distribution.

In the case that the spectral processes Y_i, $i \geq 1$, are a.s. bounded, that is,

$$\sup_{x\in\mathcal{X}} Y_i(x) \leq C \quad a.s. \tag{1.6}$$

for some constant $C > 0$, the product $(\sum_{j=1}^{k+1} E_j)^{-1} Y_{k+1}$ cannot contribute to the pointwise maximum in (1.5) if

$$\frac{C}{\sum_{j=1}^{k+1} E_j} \leq \inf_{x\in\mathcal{X}} \left(\max_{i\geq 1} \frac{Y_i(x)}{\sum_{j=1}^i E_j} \right). \tag{1.7}$$

(cf. Schlather, 2002; Oesting et al., 2013). As the points $\{(\sum_{j=1}^i E_j)^{-1}\}_{i\geq 1}$ are in a descending order, this fact allows us to write the process Z as the pointwise maximum over a finite number of functions.

Proposition 1.2.1. *(analogous to Schlather, 2002, Thm. 4) Let $E_i \sim_{iid} \mathrm{Exp}(1)$, $i \geq 1$, and, independently of $\{E_i\}_{i\geq 1}$, let Y_i, $i \geq 1$, be independent copies of a stochastic process Y satisfying (1.6) for some $C > 0$. Then,*

$$\max_{i=1}^N \left(\left(\sum_{j=1}^i E_j \right)^{-1} Y_i(x) \right) = \max_{i\geq 1} \left(\left(\sum_{j=1}^i E_j \right)^{-1} Y_i(x) \right), \qquad x \in \mathcal{X},$$

where N is an a.s. finite random number N, defined by

$$N = \min \left\{ k \geq 1 : \ \frac{C}{\sum_{j=1}^{k+1} E_j} \leq \inf_{x\in\mathcal{X}} \left(\max_{i=1}^k \frac{Y_i(x)}{\sum_{j=1}^i E_j} \right) \right\}.$$

In particular, the process Z given by (1.4) satisfies $Z(\cdot) =_d \max_{i=1}^N \frac{Y_i(\cdot)}{\sum_{j=1}^i E_j}$.

Thus, the process Z can be simulated exactly in finite time by the following algorithm.

Algorithm 1.2.2. Simulation of a max-stable process (1.4) **with spectral function bounded by** C
Set $Z(x) = 0$, $x \in \mathcal{X}$, *and simulate* $\zeta^{-1} \sim \text{Exp}(1)$.
while $(\zeta C > \inf_{x\in\mathcal{X}} Z(x))$ {
    Simulate $Y \sim \nu$.
    Update $Z(x)$ *by* $\max\{Z(x), \zeta Y(x)\}$ *for all* $x \in \mathcal{X}$.
    Simulate $E \sim \text{Exp}(1)$ *and update* ζ^{-1} *by* $\zeta^{-1} + E$.
}
Return Z.

For many examples of processes represented via stochastic processes, condition (1.6) is not satisfied. In this case, Schlather (2002) proposes to approximate the process by choosing some constant C^* and applying Algorithm 1.2.2 with $C = C^*$. For an accurate approximation, C^* should be chosen large enough such that $\mathbb{P}(\sup_{x\in\mathcal{X}} Y(x) > C^*)$ is small. However, the larger C^* is, the more iterations of the algorithm are needed until the stopping criterion is met. Thus, the choice of C^* is a trade-off between simulation accuracy and running time. We will deal with this question in more detail in Section 1.4.

One way to handle the difficulties associated with the choice of an upper bound C^* might be the choice of a different but stochastically equivalent spectral representation, that is, a spectral representation that yields a max-stable process with the same distribution. Note that, by Corollary 9.4.5 in de Haan and Ferreira (2006), any sample-continuous max-stable process possesses a spectral representation satisfying $\sup_{x\in\mathcal{X}} Y(x) = c$ a.s. for some positive constant c. In particular, condition (1.6) is met and, thus, the process can be simulated exactly using the above algorithm. We will discuss the construction of such a representation and its effects on simulation in Section 1.3.

1.2.2 Mixed Moving Maxima Processes

As a second class of max-stable processes, we consider the class of mixed moving maxima processes on $\mathbb{R}^d$ (see Schlather, 2002; Stoev and Taqqu, 2005, for example). Here, let $\{(\zeta_i, S_i)\}_{i\geq 1}$ be the points of a Poisson point process on $(0,\infty) \times \mathbb{R}^d$ with intensity measure $\zeta^{-2}\mathrm{d}\zeta \times \mathrm{d}s$. Independently, let $F_i \sim_{iid} F$, $i \geq 1$, for some nonnegative random function F on $\mathbb{R}^d$ satisfying $\mathbb{E}\left(\int_{\mathbb{R}^d} F(x)\,\mathrm{d}x\right) = 1$. Then, the mixed moving maxima process

$$Z(x) = \max_{i\geq 1} \zeta_i F_i(x - S_i), \quad x \in \mathcal{X}, \tag{1.8}$$

is a stationary max-stable process with standard Fréchet margins. Note that the class of mixed moving maxima processes contains the processes considered by Smith (1990) with F being a deterministic function, for instance, a Gaussian density function. The work of Smith (1990) also provides an interpretation of mixed moving maxima as models for storms, where ζ_i is perceived as the strength, S_i as the center and F_i as the shape of a storm.

In contrast to the representation via stochastic processes considered in Subsection 1.2.1, here, the associated spectral measure ν, given by

$$\nu(A) = \int_{\mathbb{R}^d} \mathbb{P}(F(\cdot - s) \in A)\, \mathrm{d}s, \quad A \subset \mathcal{C} \text{ Borel},$$

is infinite. Due to this fact, the collection $\{\zeta_i\}_{i\geq 1}$ of first components of the points $\{(\zeta_i, S_i)\}_{i\geq 1}$ cannot be simulated in a descending order as the number of ζ_i, $i \geq 1$, with $a \leq \zeta_i \leq b$ is infinite for all $0 < a < b$. However, this number becomes finite if we restrict ourselves to those points whose second component is in some compact set.

Note that such a restriction can be made without affecting the corresponding max-stable process Z if the shape functions are a.s. supported in some compact domain only, i.e., if we have

$$\mathbb{P}(F(x) = 0 \text{ for all } x \in \mathbb{R}^d \setminus b(o, R)) = 1 \tag{1.9}$$

for some $R > 0$ where $b(o, R)$ denotes a d-dimensional ball around the origin with radius R. In this case, the process $\zeta_i F_i(\cdot - S_i)$ cannot contribute to the maximum $\{Z(X) : \ x \in \mathcal{X}\}$ if $S_i \notin K \oplus b(o, R)$ where $A \oplus B = \{a + b : \ a \in A,\, b \in B\}$ for $A, B \subset \mathbb{R}^d$. Thus, instead of considering all points $\{(\zeta_i, S_i)\}_{i\geq 1}$, the points $\{(\zeta_i, S_i) : \ S_i \in \mathcal{X} \oplus b(o, R)\}_{i\geq 1}$, i.e. the points of the Poisson point process restricted to $(0, \infty) \times (\mathcal{X} \oplus b(o, R))$, are sufficient to simulate the process $\{Z(x),\, x \in \mathcal{X}\}$. These points can be simulated in the following way (cf. Schlather, 2002, Lemma 3): Let $E_j \sim_{iid} \mathrm{Exp}(1)$, $j \geq 1$, and, independently of $\{E_j\}_{j\geq 1}$, let S_i, $i \geq 1$, be independent random variables uniformly distributed on $\mathcal{X} \oplus b(o, R)$, denoted by $S_i \sim_{iid} \mathrm{Unif}(\mathcal{X} \oplus b(o, R))$. Then, the points

$$\left\{ \left(|\mathcal{X} \oplus b(o, R)| \left(\textstyle\sum_{j=1}^{i} E_i \right)^{-1}, S_i \right) \right\}_{i\geq 1}$$

form a Poisson point process on $(0, \infty) \times (\mathcal{X} \oplus b(o, R))$ with the desired intensity measure, where $|\cdot|$ denotes the Lebesgue measure. Thus, the mixed moving maxima process (1.8) can be written as the maximum over a finite number of functions provided that the shape function F is bounded and satisfies (1.9).

Proposition 1.2.3. *(Schlather, 2002, Thm. 4) Let F_i, $i \geq 1$, be independent copies of some stochastic process F that satisfies* (1.9) *for some $R > 0$ and*

$$\sup_{x\in\mathbb{R}^d} F(x) \leq C \quad a.s. \tag{1.10}$$

for some $C > 0$. Independently of $\{F_i\}_{i\geq 1}$, let $E_i \sim_{iid} \mathrm{Exp}(1)$, $i \geq 1$, and $S_i \sim_{iid} \mathrm{Unif}(\mathcal{X} \oplus b(o, R))$ be independent sequences. Then, the mixed moving maxima process $\{Z(x),\, x \in \mathcal{X}\}$ defined in (1.8) *satisfies*

$$Z(\cdot) =_d \max_{i=1}^{N} \frac{|\mathcal{X} \oplus b(o, R)|}{\sum_{j=1}^{i} E_j} F_i(\cdot - S_i)$$

for an a.s. finite number N defined by

$$N = \min \left\{ k \geq 1 : \ \frac{C}{\sum_{j=1}^{k+1} E_j} \leq \inf_{x\in\mathcal{X}} \left(\max_{i=1}^{k} \frac{F_i(x - S_i)}{\sum_{j=1}^{i} E_j} \right) \right\}.$$

This result allows for the following implementation of an exact simulation procedure.

Algorithm 1.2.4. Simulation of a max-stable process (1.8) **with shape function supported within** $b(0,R)$ **and bounded by** C
Set $Z(x)=0$, $x\in\mathcal{X}$, *and simulate* $\zeta^{-1}\sim\mathrm{Exp}(1)$.
while $(\zeta C > \inf_{x\in\mathcal{X}} Z(x)/|\mathcal{X}\oplus b(o,R)|)$ {
Simulate $F\sim\mathbb{P}(F\in\cdot)$ *and* $S\sim\mathrm{Unif}(\mathcal{X}\oplus b(o,R))$.
Update $Z(x)$ *by* $\max\{Z(x), |\mathcal{X}\oplus b(o,R)|\cdot\zeta\cdot F(x-S)\}$ *for all* $x\in\mathcal{X}$.
Simulate $E\sim\mathrm{Exp}(1)$ *and update* ζ^{-1} *by* $\zeta^{-1}+E$.
}
Return Z.

If not both condition (1.9) and (1.10) are met, similarly to the case of a representation via stochastic processes, Schlather (2002) proposes an approximation. We choose $R^*>0$ and $C^*>0$ such that $\mathbb{P}(\sup_{x\in\mathbb{R}^d} F(x) > C^*)$ is small and the shape function F is negligible outside $b(o,R)$ and apply Algorithm 1.2.4 with $R=R^*$ and $C=C^*$. Again, the choice of R^* and C^* is a trade-off between accuracy and running time of the simulation algorithm. We will further address this issue in Section 1.4 providing some error bounds.

1.3 The Choice of the Spectral Representation

In this section, we will discuss the choice of the (non-unique) spectral representation of a max-stable process and its effects on simulation. We will consider several transformations that allow for switching from one spectral to another.

At first, we review a class of transformations presented in Oesting et al. (2013) leading to several equivalent representations via stochastic processes. We start with a max-stable process Z with general representation (1.1) and spectral measure ν. Let g be a probability density function with respect to ν, i.e. $g\geq 0$ and $\int_{\mathcal{C}} g(f)\,\nu(\mathrm{d}f)=1$, such that

$$\nu\left(\{f\in\mathcal{C}:\, g(f)=0,\, \sup_{x\in\mathcal{X}} f(x)>0\}\right)=0.$$

Then, we obtain that

$$Z(x) =_d \max_{i\geq 1} \frac{1}{\sum_{j=1}^{i} E_j}\frac{Y_i^*(x)}{g(Y_i^*)},\quad x\in\mathcal{X}, \tag{1.11}$$

where Y_i^*, $i\geq 1$, are independent and identically distributed according to the probability measure $g\nu$, i.e. $\mathbb{P}(Y_i^*\in A)=\int_{\mathcal{C}}\mathbf{1}_A(f)g(f)\,\nu(\mathrm{d}f)$ for all Borel sets $A\subset\mathcal{C}$, (Oesting et al., 2013, Prop. 2.1). In particular, the transformed spectral functions $Y_i^*/g(Y_i^*)$ can be seen as independent and identically distributed processes. Thus, (1.11) is a representation of Z via stochastic processes.

Similarly to Subsection 1.2.1, the representation via stochastic processes allows us to give some stopping rule for the simulation. Following Oesting et al. (2013), this criterion will in general be sharper than the one presented in Subsection 1.2.1 as it is based on a pointwise bound instead of an overall bound: A function $(\sum_{j=1}^{k} E_j)^{-1} Y_k^*(x)/g(Y_k^*)$ cannot contribute to the pointwise maximum in (1.11) if

$$\frac{1}{\sum_{j=1}^{k+1} E_j} \operatorname*{ess\,sup}_{f \in \mathcal{C}} \frac{f(x)}{g(f)} \leq \max_{i \geq 1} \frac{1}{\sum_{j=1}^{i} E_j} \frac{Y_i^*(x)}{g(Y_i^*)} \quad \text{for all } x \in \mathcal{X},$$

or, equivalently,

$$\sum_{j=1}^{k+1} E_j \geq \sup_{x \in \mathcal{X}} \operatorname*{ess\,sup}_{f \in \mathcal{C}} \frac{f(x)}{g(f) Z^{(k)}(x)} \tag{1.12}$$

where

$$Z^{(k)}(x) = \max_{i=1}^{k} \frac{1}{\sum_{j=1}^{i} E_j} \frac{Y_i^*(x)}{g(Y_i^*)}, \quad x \in \mathcal{X},$$

and ess sup denotes the essential supremum with respect to the transformed measure $g\nu$. Thus, as $\inf_{x \in \mathcal{X}} Z(x) > 0$ a.s., the representation (1.11) allows for an exact simulation of Z in a.s. finite time if and only if g satisfies

$$\sup_{x \in \mathcal{X}} \operatorname*{ess\,sup}_{f \in \mathcal{C}} \frac{f(x)}{g(f)} < \infty. \tag{1.13}$$

Oesting et al. (2013) focus on a specific choice of g that satisfies (1.13) — the so-called *normalized spectral representation*. This representation — whose existence is shown by de Haan and Ferreira (2006), Cor. 9.4.5 — is a representation via stochastic processes (1.11) and is characterized by the fact that the stochastic processes Y_i, $i \geq 1$, (which correspond to $Y_i^*/g(Y_i^*)$ in representation (1.11)) satisfy

$$\sup_{x \in \mathcal{X}} Y_i(x) = c \quad a.s. \tag{1.14}$$

for some $c > 0$. In representation (1.11), this corresponds to the choice $g(f) = c^{-1} \sup_{x \in \mathcal{X}} f(x)$ where

$$c = \int_{\mathcal{C}} \sup_{x \in \mathcal{X}} f(x)\, \nu(\mathrm{d}f) = -\log \mathbb{P}\left(\sup_{x \in \mathcal{X}} Z(x) \leq 1\right)$$

which ensures that g is a probability density with respect to ν as well as (1.14) by which it is determined uniquely. Note that $c < \infty$ if and only if $\sup_{x \in \mathcal{X}} Z(x) < \infty$ a.s. (cf. Resnick and Roy, 1991) which holds as Z is sample-continuous. Further, the distribution of the spectral functions $Y_i^*/g(Y_i^*)$ is uniquely defined by (1.14) (cf. Oesting et al., 2013, Prop. 2.5). In particular, the distribution does not depend on the initial choice of ν.

Due to (1.14), the normalized spectral representation allows for an exact simulation in a.s. finite time. Although in general being slightly less precise

than the stopping rule (1.12) with $g(f) = c^{-1} \sup_{x\in\mathcal{X}} f(x)$, in this case, in practice, the simulation is stopped if

$$\sum_{j=1}^{k+1} E_j \geq \frac{c}{\inf_{x\in\mathcal{X}} Z^{(k)}(x)}, \tag{1.15}$$

that is, simulation is performed according to Algorithm 1.2.2 with $C = c$.

Although simulation via the normalized spectral representation is exact and, as we will see in Section 1.4, seems to be quite efficient, for some models, the implementation may be difficult in practice due to the transformed measure $g\nu$. While the original spectral representation is usually chosen such that the spectral function can be simulated at rather little cost, this is not necessarily the case any more for the functions $Y_i^* \sim g\nu$ from representation (1.11). Thus, in view of the simulation efficiency, it may be useful to use a different representation. Engelke et al. (2014) present transformations that allow to switch between a representation via stochastic processes (1.4) and a mixed moving maxima representation (1.8). While a mixed moving maxima representation can always be transformed into a representation via stochastic processes via a transformation of the same type as in (1.11), the existence of a mixed moving maxima representation is linked to further assumptions on the spectral process $Y \sim \nu$ defined on $\mathbb{R}^d$. According to Kabluchko et al. (2009) and Engelke et al. (2014) sufficient conditions are:

(i) $\mathbb{E}(Y(x)) = 1$ for all $x \in \mathbb{R}^d$

(ii) $\lim_{\|x\|\to\infty} Y(x) = 0$ a.s.

(iii) $\mathbb{E}(\sup_{x\in K} Y(x)) < \infty$ for all compact sets $K \subset \mathbb{R}^d$

If all these conditions are satisfied, the max-stable process (1.4) can be written as a mixed moving maxima process (1.8) with shape function $F(\cdot) = (\mathbb{E}(\int_{\mathbb{R}^d} \tilde{F}(x)\,\mathrm{d}x))^{-1}\tilde{F}(\cdot)$ where the distribution of $\tilde{F}$ is given by

$$\mathbb{P}(\tilde{F} \in A) = \frac{\int_0^\infty m\mathbb{P}(Y(\cdot+\tau)/m \in A,\, \tau \in K \mid M = m)\,\mathbb{P}(M \in \mathrm{d}m)}{\int_0^\infty m\mathbb{P}(\tau \in K \mid M = m)\,\mathbb{P}(M \in \mathrm{d}m)} \tag{1.16}$$

for any Borel set $A \subset C(\mathbb{R}^d)$ (Engelke et al., 2014, Thm. 4.3). Here, $K \subset \mathbb{R}^d$ is an arbitrary compact set and M and τ are random variables defined by $M = \max_{x\in\mathbb{R}^d} Y(x)$ and $\tau = \inf\{\arg\max_{x\in\mathbb{R}^d} Y(x)\}$, respectively. Note that, with probability one, the maximum of the shape function F has the value $\mathbb{E}(\int_{\mathbb{R}^d} \tilde{F}(x)\,\mathrm{d}x))^{-1}$ and is attained at the origin. Thus, it is suitable to simulate the process via Algorithm 1.2.4 even though the support of F may be unbounded. In general, the distribution of the shape function given by (1.16) is difficult to handle. However, in some cases, it allows for simulation (see Subsection 1.5.3 for some examples).

1.4 Measures of Simulation Efficiency and Quality

In this section, we will investigate the efficiency and quality of the simulation procedures introduced above. Following Dombry and Éyi-Minko (2012) and Dombry and Éyi-Minko (2013), we separate the set of Poisson points $\{\zeta_i, \psi_i\}_{i\geq 1}$ from (1.1) into those processes that contribute to the maximum Z and those that do not. To this end, we define the set of *extremal functions*

$$\Phi^+ = \{(\zeta_k, \psi_k) : \zeta_k\psi_k(x) = \max_{i\geq 1} \zeta_i\psi_i(x) \text{ for some } x \in \mathcal{X}\}$$

and the set of *subextremal functions*

$$\Phi^- = \{(\zeta_k, \psi_k) : \zeta_k\psi_k(x) < \max_{i\geq 1} \zeta_i\psi_i(x) \text{ for all } x \in \mathcal{X}\}.$$

Note that both Φ^+ and Φ^- form point processes (cf. Dombry and Éyi-Minko, 2012). In view of these definitions, a realization that is obtained by some simulation procedure can be seen as correct if all extremal functions are taken into consideration, and a simulation algorithm is an exact algorithm if the resulting realizations are correct with probability one. Thus, an appropriate measure quality of an approximative procedure is the probability of producing incorrect realizations. Besides providing accurate realizations, a simulation algorithm should also be efficient, that is the number of subextremal functions taken into consideration should be minimal.

1.4.1 Simulation Efficiency

We first investigate the efficiency of an exact algorithm which we measure in terms of the expected number of spectral functions that need to be simulated until a stopping criterion is satisfied.

Oesting et al. (2013) consider this value as criterion for a good choice of a spectral representation, that is, the choice of the density g in representation (1.11). In this case, according to the stopping rule (1.12), on average

$$Q_g = \mathbb{E}\min\left\{m \in \mathbb{N} : \operatorname*{ess\,sup}_{f\in\mathcal{C}} \sup_{x\in\mathcal{X}} \frac{f(x)}{g(f)Z^{(m)}(x)} \leq \sum\nolimits_{j=1}^{m+1} E_j\right\}$$

spectral functions have to be considered. Decomposing the considered functions into extremal and subextremal functions, this number can be computed

$$Q_g = \mathbb{E}\left(\operatorname*{ess\,sup}_{f\in\mathcal{C}} \sup_{x\in\mathcal{X}} \frac{f(x)}{g(f)Z(y)}\right). \tag{1.17}$$

Thus, a transformation that yields the most efficient simulation algorithm, can be found by minimizing (1.17) with respect to g. However, as this optimization problem is very difficult, Oesting et al. (2013) present a closely

related class of replacement problems, which they show to be solved uniquely by the normalized spectral representation, i.e. by $g^*(f) = c^{-1} \sup_{x\in\mathcal{X}} f(x)$. For this choice, the expression (1.17) can be bounded by $c\mathbb{E}[(\inf_{x\in\mathcal{X}} Z(x))^{-1}]$ which corresponds to the number of spectral functions considered according to Algorithm 1.2.2 with $C = c$.

Adapting the stopping rules, we can modify the proof of Prop. 4.8 in Oesting et al. (2013) to obtain the expected number of functions considered in the exact procedures given by Algorithms 1.2.2 and 1.2.4, respectively.

Proposition 1.4.1. *Let $\{E_j\}_{j\geq 1}$ be independent standard exponentially distributed random variables.*

1. *Independently of the E_j's, let Y_j, $j \geq 1$, be independent copies of a nonnegative stochastic process Y satisfying $\mathbb{E}Y(x) = 1$ for all $x \in \mathcal{X}$ and $\sup_{x\in\mathcal{X}} Y(x) \leq C$ a.s. for some $C > 0$. Further, let Z be defined by (1.4). Then, we have*

$$\mathbb{E}\min\left\{k \geq 1 : \frac{C}{\sum_{j=1}^{k+1} E_j} \leq \inf_{x\in\mathcal{X}} \max_{i=1}^{k} \frac{Y_i(x)}{\sum_{j=1}^{i} E_j}\right\} = C\mathbb{E}\left[\left(\inf_{x\in\mathcal{X}} Z(x)\right)^{-1}\right].$$

2. *Independently of the E_j's, let F_j, $j \geq 1$, be independent copies of a nonnegative stochastic process F satisfying $\mathbb{E}\int_{\mathcal{X}} F(x)\,\mathrm{d}x = 1$, $\sup_{x\in\mathcal{X}} F(x) \leq C$ a.s. for some $C > 0$ and (1.9) for some $R > 0$. Further, let $S_j \sim_{iid} \mathrm{Unif}(\mathcal{X} \oplus b(o, R))$, $j \geq 1$, and Z be defined by (1.8). Then, we have*

$$\begin{aligned}&\mathbb{E}\min\left\{k \geq 1 : \frac{C}{\sum_{j=1}^{k+1} E_j} \leq \inf_{x\in\mathcal{X}} \max_{i=1}^{k} \frac{F_i(x - S_i)}{\sum_{j=1}^{i} E_j}\right\}\\ &= C \cdot |\mathcal{X} \oplus b(o, R)| \cdot \mathbb{E}\left[\left(\inf_{x\in\mathcal{X}} Z(x)\right)^{-1}\right].\end{aligned}$$

Remark 1.4.2. *By Thm. 2.2 in Dombry and Éyi-Minko (2012), the quantity $\mathbb{E}\big[\left(\inf_{x\in\mathcal{X}} Z(x)\right)^{-1}\big]$ is finite for any compact set $\mathcal{X} \subset \mathbb{R}^d$ and any sample-continuous max-stable process Z with unit Fréchet margins.*

1.4.2 Simulation Quality

In this subsection, we consider measures for the quality of simulation algorithms that are not exact. In particular, we provide error estimates for Algorithms 1.2.2 and 1.2.4 in the case that the underlying assumptions are not met such that an approximative stopping rule is applied. Here, a realization produced by this algorithm is not correct if there exists at least one extremal function that is not taken into consideration by the algorithm, i.e. some $(\zeta_i, \psi_i) \in \Phi$ which already satisfies the stopping criterion. Using Slivnyak's formula from Poisson point process theory (cf. Stoyan et al., 1995), we obtain the following assessments for the probability of obtaining an incorrect realization when applying Algorithms 1.2.2 and 1.2.4 with $C = C^*$ and $R = R^*$, respectively.

Proposition 1.4.3. *Let Z be a max-stable process with spectral representation* (1.4)*. Then, for any $C^* > 0$, we have*

$$\begin{aligned} &\mathbb{P}\left(\exists(\zeta_i, Y_i) \in \Phi^+ : \zeta_i C^* < \inf_{x\in\mathcal{X}} \max_{j=1}^{i-1} \zeta_j Y_j(x)\right) \\ &\leq \sqrt{\mathbb{E}\left(\sup_{x\in\mathcal{X}} \left(Y(x)/Z(x)\right)^2\right)} \cdot \sqrt{\mathbb{P}\left(\sup_{x\in\mathcal{X}} Y(x) > C^*\right)}. \end{aligned} \tag{1.18}$$

Proof. First, we note that a point $(\zeta_i, Y_i) \in \Phi^+$ that is not considered due to the stopping criterion necessarily satisfies $\sup_{x\in\mathcal{X}} Y(x) > C^*$. Thus, we have

$$\begin{aligned} &\mathbb{P}\left(\exists(\zeta_i, Y_i) \in \Phi^+ : \zeta_i C^* < \inf_{x\in\mathcal{X}} \max_{j=1}^{i-1} \zeta_j Y_j(x)\right) \\ &\leq \mathbb{E}\left(\sum\nolimits_{(\zeta,Y)\in\Phi} \mathbf{1}_{\{\zeta Y(x) \geq \max_{(\tilde{\zeta},\tilde{Y})\in\Phi\setminus\{(\zeta,Y)\}} \tilde{\zeta}\tilde{Y}(x) \text{ for some } x\in\mathcal{X}\}} \mathbf{1}_{\{\sup_{x\in\mathcal{X}} Y(x) > C^*\}}\right) \\ &= \int_0^\infty \zeta^{-2} \mathbb{E}\left(\mathbf{1}_{\{\zeta Y(x) > Z(x) \text{ for some } x\in\mathcal{X}\}} \mathbf{1}_{\{\sup_{x\in\mathcal{X}} Y(x) > C^*\}}\right) \mathrm{d}\zeta \\ &= \mathbb{E}\left(\sup_{x\in\mathcal{X}} \frac{Y(x)}{Z(x)} \mathbf{1}_{\{\sup_{x\in\mathcal{X}} Y(x) > C^*\}}\right), \end{aligned}$$

where we use Slivnyak's formula (Stoyan et al., 1995) to obtain the equality of the second and the third lines. The assertion of the proposition is obtained by applying the Cauchy-Schwarz inequality. □

For the error estimate for Algorithm 1.2.4, we assume that the shape function F is uniformly bounded by some constant $C > 0$, which is the case for all the examples considered in this chapter. In the case that F is unbounded, the additional error can be assessed in a similar way as in Proposition 1.4.3.

Proposition 1.4.4. *Let Z be a max-stable process with spectral representation* (1.8)*. Further assume that the corresponding shape function F satisfies* (1.10)*. Then, for any $R^* > 0$, we have*

$$\begin{aligned} &\mathbb{P}\Big(\exists(\zeta_i, S_i, F_i) \in \Phi^+ : S_i \notin \mathcal{X} \oplus b(o, R^*)\Big) \\ &\leq \mathbb{E}\left[\left(\inf_{x\in\mathcal{X}} Z(x)\right)^{-1}\right] \cdot \int_{\mathbb{R}^d\setminus(\mathcal{X}\oplus b(o,R^*))} \mathbb{E}\left(\sup_{x\in\mathcal{X}} F(x-s)\right) \mathrm{d}s. \end{aligned} \tag{1.19}$$

Proof. Using Slivnyak's Theorem (Stoyan et al., 1995), we obtain that

$$\begin{aligned} &\mathbb{P}\Big(\exists(\zeta_i, S_i, F_i) \in \Phi^+ : S_i \notin \mathcal{X} \oplus b(o, R^*)\Big) \\ &\leq \mathbb{E}\left(\sum\nolimits_{(\zeta,F(\cdot-S))\in\Phi} \mathbf{1}_{\zeta F(x-S) \geq \max_{(\tilde{\zeta},\tilde{F}(\cdot-\tilde{S}))\in\Phi\setminus\{(\zeta,F(\cdot-S))\}} \tilde{\zeta}\tilde{F}(x-\tilde{S}) \text{ for some } x\in\mathcal{X}}\right) \\ &= \int_{\mathbb{R}^d\setminus(\mathcal{X}\oplus b(o,R^*))} \int_0^\infty \zeta^{-2} \mathbb{E}\left(\mathbf{1}_{\zeta F(x-S) \geq Z(x) \text{ for some } x\in\mathcal{X}}\right) \mathrm{d}\zeta \, \mathrm{d}s \end{aligned}$$

$$= \int_{\mathbb{R}^d \setminus (\mathcal{X} \oplus b(o,R^*))} \mathbb{E}\left(\sup_{x\in\mathcal{X}} \frac{F(x-s)}{Z(x)}\right) \mathrm{d}s.$$

The assertion of the proposition follows from the fact that $\sup_{x\in\mathcal{X}} \frac{F(x-s)}{Z(x)} \leq (\sup_{x\in\mathcal{X}} F(x-s)) \cdot (\inf_{x\in\mathcal{X}} Z(x))^{-1}$. □

Remark 1.4.5. *Note that the integral* $\int_{\mathbb{R}^d} \mathbb{E}\,(\sup_{x\in\mathcal{X}} F(x-s))\,\mathrm{d}s$ *is finite if* Z *has continuous sample paths (Resnick and Roy, 1991). Thus, indeed, the error bound tends to zero as* $R^* \to \infty$.

Besides using these error estimates, there are also other diagnostic tools to assess the quality of a simulation algorithm. In particular, it can be checked whether the marginal distributions are reproduced correctly. As an example one can calculate the Kolmogorov-Smirnov distance between the simulated and the theoretical marginal distributions as Oesting et al. (2012) did in a simulation study to compare different simulation algorithms for Brown-Resnick processes. Also graphical tools, like Q-Q plots for the marginal distribution, or a plot of the extremal coefficient function θ which, for a stationary max-stable process Z, is defined by

$$\mathbb{P}(Z(t+h) \leq x,\, Z(t) \leq x) = \mathbb{P}(Z(t) \leq x)^{\theta(h)}, \quad h \in \mathbb{R}^d,$$

(Schlather and Tawn, 2003), can be used. See Subsection 1.5.2, for an example.

1.5 Examples

In this section, we discuss the choice of an accurate simulation procedure for several examples, including some of the most popular models of max-stable processes. For more details on these models, see Chapter ??.

1.5.1 Moving Maxima Processes

As the first example, we consider moving maxima processes, i.e. mixed moving maxima processes (1.8) with a deterministic shape function F. Of particular interest are the processes devised by Smith (1990) who uses probability densities as shape functions. If such a density function f is radially decreasing, the transformed Lebesgue density $g(f) = c^{-1} \sup_{x\in\mathcal{X}} f(x)$ from the normalized spectral representation allows for convenient sampling (cf. Oesting et al., 2013, for explicit formulae). Thus, the normalized spectral representation can be used for an exact simulation. Simulation studies in Oesting et al. (2013) for the case of f being a 1- or 2-dimensional Gaussian density show that the usage of the normalized spectral representation also yields remarkable improvements with respect to the number of considered spectral functions in comparison to

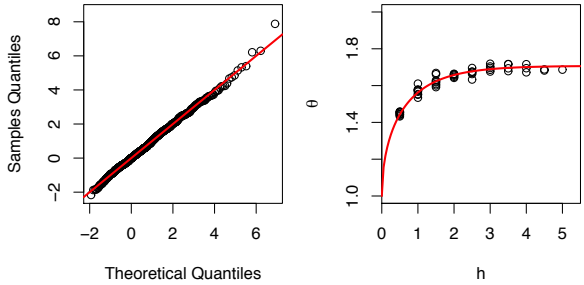

FIGURE 1.2
Diagnostic plots based on 1000 realizations of an extremal Gaussian process simulated via Algorithm 1.2.2 with $C = 5$. Left: Q-Q plot of the empirical distribution of $\log Z(0)$ against the standard Gumbel distribution. Right: Empirical extremal coefficients in comparison to the theoretical extremal coefficient function (red line).

Schlather's (2002) algorithm even though the latter one provides an approximation only. Thus, simulation via the normalized spectral representation is preferable both with respect to simulation accuracy and costs.

1.5.2 Extremal Gaussian and Extremal t Processes

Secondly, we consider extremal Gaussian processes (Schlather, 2002), i.e. processes of the form

$$Z(x) = \max_{i\geq 1} \zeta_i \sqrt{2\pi} \max\{0, W_i(x)\}, \quad x \in \mathcal{X},$$

where W_i, $i \geq 1$, are independent copies of some stationary standard Gaussian process W with correlation function $\rho(h)$, independently from the Poisson point process $\{\zeta_i\}_{i\geq 1}$ with intensity $\zeta^{-2}\mathrm{d}\zeta$.

Here, for simulation based on the normalized spectral representation, one has to sample from the modified law $c^{-1}\max\{0, \sup_{x\in\mathcal{X}} w(x)\}\mathbb{P}(W \in \mathrm{d}w)$. Although this can be done by MCMC methods, such a sampling procedure is very complex and time-consuming compared to sampling from W. Thus, we consider approximations via Algorithm 1.2.2. According to the approximation procedure described in Subsection 1.2.1, we choose some value C^* such that $\mathbb{P}(\sup_{x\in\mathcal{X}} \sqrt{2\pi}W(x) > B)$ is small and run Algorithm 1.2.2 with $C = C^*$.

To show the performance of the approximation procedure, we choose the bound $C^* = 5$ and simulate 1000 realizations of an extremal Gaussian process on $\{0, 0.5, \ldots, 4.5, 5\}$ based on Gaussian processes W_i with correlation function $\rho(h) = \exp(-|h|)$. Figure 1.5.2 shows a Q-Q plot of the empirical distribution of $\log Z(0)$ against the standard Gumbel distribution and the empirical extremal coefficients in comparison to the theoretical extremal coefficient function $\theta(h) = 1 + \sqrt{(1-\rho(h))/2}$. As both the Q-Q plot and the

extremal coefficient indicate, the approximation is quite accurate even though the bound $C = 5$ is rather small (this corresponds to a bound $B \approx 2$ for W).

The class of extremal Gaussian processes is generalized by extremal-t processes (Opitz, 2013)

$$Z(x) = \max_{i \geq 1} \zeta_i c_\alpha \max\{0, W_i(x)\}^\alpha, \quad x \in \mathcal{X},$$

where $c_\alpha = \sqrt{\pi} 2^{-(\alpha-2)/2} \Gamma((\alpha+1)/2)^{-1}$ for $\alpha > 0$. For small or moderate values of α, similar techniques as in the case of the extremal Gaussian process are suitable for simulation. If α gets large, the extremal t-process resembles a Brown-Resnick process which we will discuss in the following example.

1.5.3 Brown-Resnick Processes

As the last example, we consider the challenging case of Brown-Resnick processes as defined 1.3. Kabluchko et al. (2009) show that the Brown-Resnick process is stationary and that its law – and, thus, the choice of an appropriate simulation procedure – depends on γ only. Therefore, Z is called Brown-Resnick process associated to the semi-variogram γ.

First, we note that, as for extremal Gaussian processes, the simulation of normalized spectral functions is very complex, but could be done by MCMC methods. Thus, in the following, we will focus on alternative approaches.

In the case that W is a stationary process, that is, Z is a so-called geometric Gaussian process (Davison et al., 2012), the semi-variogram is bounded and the variance function is constant. Thus, the process can be approximated by Algorithm 1.2.2 with an appropriate value C which, however, may be much larger than in the Gaussian case, in particular, if the variance σ^2 is large. As W is stationary, so are all finite approximations.

If, however, γ (and, thus, also the variance function) is unbounded, the single spectral functions $Y_i(x) = \exp(W_i(x) - \sigma^2(x)/2)$ and the finite approximations exhibit clear non-stationary trends. Similarly to the example in Section 1.1 (Figure 1.1) where a fixed number of spectral functions is considered, these problems also occur in case of Algorithm 1.2.2. Figure 1.5.3 shows realizations of the original Brown-Resnick process (Brown and Resnick, 1977) with W being a standard Brownian motion, i.e. a Brown-Resnick process associated to semi-variogram $\gamma(h) = \frac{1}{2}|h|$, for several values of C. Note that the realizations look non-stationary even for large values of C.

Oesting et al. (2012) introduce several equivalent representations in order to generate approximations that indicate stationarity. For example, they consider random shifts of the spectral functions. Let ζ_i, W_i, $i \geq 1$, be as above, and, independently from ζ_i, W_i, let X_i, $i \geq 1$, be independent random vectors in $\mathbb{R}^d$ distributed according to some measure μ. Then, for the Brown-Resnick process Z associated to the semi-variogram γ, we have

$$Z(x) =_d \max_{i \geq 1} \zeta_i \exp\left(W_i(x - X_i) - \sigma^2(x - X_i)/2\right), \quad x \in \mathcal{X}. \tag{1.20}$$

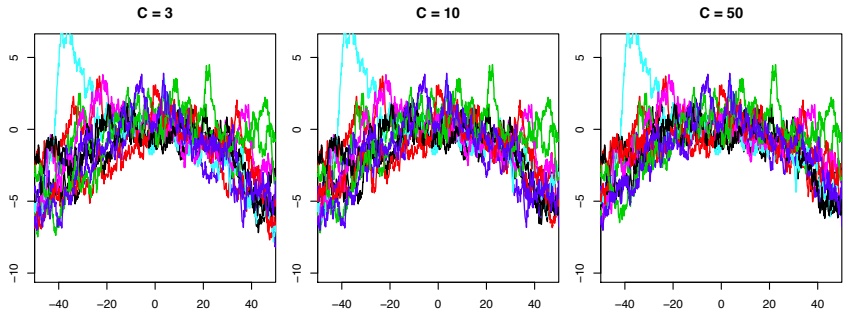

FIGURE 1.3
Ten approximations of $\log Z$ on the interval $[-50, 50]$ by applying Algorithm 1.2.2 with $C = 3$, 10, 25 (from left to right). Here, Z is a Brown-Resnick process associated to the semi-variogram $\gamma(h) = \frac{1}{2}|h|$.

By these shifts, intuitively, the trend should vanish even in finite approximations. Thus, it is worthwhile to apply Algorithm 1.2.2 to this representation with shifted spectral functions. Results based on a uniform shift in $[-50, 50]$ are illustrated in Figure 1.5.3. Indeed, the approximations look stationary. However, even for large C, the values of Z are too small in general.

Further, one can also use Algorithm 1.2.4 to simulate Brown-Resnick processes provided that they allow for a mixed moving maxima representation. By construction — apart on some effects close to the boundary as a result of neglecting the spectral functions with $S_i \notin \mathcal{X} \oplus b(o, R)$ — this algorithm leads to stationary finite approximations. As already mentioned at the end of Section 1.3, a mixed moving maxima representation exists if

$$\lim_{\|x\|\to\infty}(W(x) - \sigma^2(x)) \quad a.s. \tag{1.21}$$

By Kabluchko et al. (2009), in the case $d = 1$, condition (1.21) is satisfied if $\lim_{x\to\infty} \gamma(x)/\log x > 8$.

In general, the simulation of shape functions according to the law given by 1.16 is rather sophisticated. However, some cases allow for simplifications. For the case of the original Brown-Resnick process where W is a standard Brownian motion, Engelke et al. (2011) make use of the Markovian structure of the Brownian motion to write F as a diffusion that allows for convenient simulation. Oesting et al. (2012) consider the case of a general Brown-Resnick process on some grid $p\mathbb{Z}^d$ for some $p > 0$ with a mixed moving maxima representation where the shifts S_i are restricted to the same grid. Using the fact that, without loss of generality, the process W can be assumed to be 0 at the origin o almost surely, they show that F has the same distribution as $\lambda \exp(W(\cdot) - \gamma(\cdot)) \mid \tau = o$ where $\tau = \inf\{\arg\max_{x\in p\mathbb{Z}^d} W(\cdot) - \gamma(\cdot)\}$ and $\lambda = p^{-d}\mathbb{P}(\tau = o)$. Thus, F can be simulated via an acceptance-rejection algorithm accepting only those functions $W - \gamma$ that attain their maximum

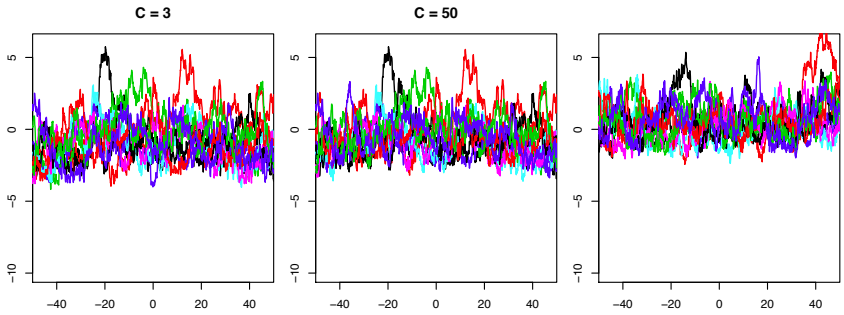

FIGURE 1.4
Ten approximations of $\log Z$ on the interval $[-50, 50]$ obtained by different procedures where Z is a Brown-Resnick process associated $\gamma(h) = \frac{1}{2}|h|$. Left/Middle: Approximations by Algorithm 1.2.2 with $C = 3$ and $C = 10$, respectively, applied to representation (1.20) with randomly shifted spectral functions. Here, the spectral functions are shifted according to a uniform distribution on $[-50, 50]$. Right: Approximations by Algorithm 1.2.4.

at the origin. As the function F is bounded by λ, Algorithm 1.2.4 can be used for simulation neglecting the spectral functions with $S_i \notin \mathcal{X} \oplus b(o, R)$. Figure 1.5.3 shows realizations of the original Brown-Resnick process simulated by this method. Indeed, the realizations look stationary and also the marginal distributions fit well. However, in the case of a dense grid, the rejection rate might be very high. Thus, Oesting et al. (2012) propose a generalization for processes on $\mathbb{R}^d$, restricting to those spectral functions whose maximum is in some specific set. By an appropriate choice of this set, the simulation error can be controlled. See Oesting et al. (2012) for more details.

In a recent publication, Dieker and Mikosch (2014) propose an alternative representation that allows for an exact simulation of Brown-Resnick processes. For an arbitrary probability measure μ on $\mathbb{R}^d$, it holds that

$$Z(x) =_d \max_{i\geq 1} \zeta_i \frac{\exp(W_i(x - X_i) - \gamma(x - X_i))}{\int_{\mathbb{R}^d} \exp(W_i(y - X_i) - \gamma(y - X_i))\, \mu(\mathrm{d}y)}, \quad x \in \mathcal{X},$$

where $\{(\zeta_i, X_i)\}_{i\geq 1}$ are the points of a Poisson point process on $(0, \infty) \times \mathbb{R}^d$ with intensity $\zeta^{-2}\, \mathrm{d}\zeta \times \mu(\mathrm{d}x)$, independently from the Gaussian processes W_i, $i \geq 1$, with $W(o) = 0$ a.s. and semi-variogram γ.

For simulating Z on some set $\{x_1, \ldots, x_n\}$, Dieker and Mikosch (2014) propose to choose $\mu = n^{-1} \sum_{k=1}^{m} \delta_{x_k}$. Noting further that $W(x-y) =_d W(x) - W(y)$ because of $W(o) = 0$ and the fact that W has stationary increments, we obtain $Z(x) =_d \max_{i\geq 1} \zeta_i Y_i(x)$ with

$$Y_i(x) = n \frac{\exp(W_i(x) - \gamma(x - T_i))}{\sum_{k=1}^{n} \exp(W_i(x_k) - \gamma(x_k - T_i))}, \quad x \in \{x_1, \ldots, x_n\}. \tag{1.22}$$

As Y_i is bounded by n, this representation allows for exact simulation on $\{x_1, \dots, x_n\}$ via Algorithm 1.2.2 with $C = n$. For a comparison of this method to an exact simulation via the normalized spectral representation, it should be mentioned that the spectral functions Y_i in (1.22) can be simulated straightforwardly while the simulation of the normalized spectral functions requires MCMC techniques. However, the bound $C = n$ for the stopping rule increases linearly in the number of simulation locations which, by Proposition 1.4.1, implies that also the number of spectral functions that have to be considered increases at least linearly. This makes it very difficult to simulate the process on a dense grid in order to approximate the continuous sample paths. Contrarily, in the case that all the simulation locations are in some bounded area K, the bound for the normalized spectral representation is always below $\mathbb{E}(\sup_{x\in K} W(x))$ and thus, due to Proposition 1.4.1, the expected number of considered spectral functions is smaller than $\mathbb{E}(\sup_{x\in K} W(x))\mathbb{E}((\inf_{x\in K} W(x))^{-1})$.

As the above discussion shows, in general, it is quite difficult to decide which spectral representation to choose for the simulation of a Brown-Resnick process. This choice depends both on the corresponding semi-variogram and on the simulation domain. Oesting et al. (2012) conduct a simulation study to compare the performance of the simulation procedures based on the original spectral representation, random shifts and the mixed moving maxima representation. We refer to their paper for more details on the results and indications for an appropriate choice of the simulation procedure.

1.6 Software Packages

Finally, we review two `R` packages that provide functions for the simulation of max-stable processes. The package `RandomFields` (Schlather et al., 2014) contains the max-stable models `RPsmith` for (mixed) moving maxima processes, `RPschlather` for extremal Gaussian processes and `RPbrownresnick` for Brown-Resnick processes (including geometric Gaussian processes). The corresponding shape function, correlation function and semi-variogram, respectively can be chosen from a large variety of basic models and combinations of them. All max-stable models can be simulated using the function `RFsimulate`. For mixed moving maxima processes, the exact simulation procedure via the normalized spectral representation (Oesting et al., 2013) is implemented. The simulation of Brown-Resnick processes is based on methods discussed in Oesting et al. (2012), namely simulation via the original spectral representation, via random shifts and via the mixed moving maxima representation. If the user does not specify the simulation method (`RPbrorig`, `RPbrshifted` and `RPbrmixed`, respectively), an appropriate procedure is chosen automatically.

Further, the package `SpatialExtremes` (Ribatet et al., 2013) allows for the simulation of max-stable processes via the function `rmaxstab`. By specifying the parameter `cov.mod`, the user can choose between different models: for example, `gauss` is used for a moving maxima process with Gaussian density function as shape function and `brown` for Brown-Resnick processes associated to a semi-variogram of the type $\gamma(h) = a\|h\|^\alpha$, $a > 0$, $0 < \alpha \leq 2$. Further, extremal Gaussian, extremal-t and geometric Gaussian processes can be simulated for some classes of correlation functions. Here, the simulation procedures used are mainly based on Schlather's (2002) algorithms. For Brown-Resnick processes, random shifts are used as well.

Acknowledgements

The work of M. Oesting was financially supported by the ANR project McSim. The authors thank Liliane Bel, Christian Lantuéjoul and Martin Schlather for numerous fruitful discussions.

References

Brown, B. M. and Resnick, S. I. (1977), "Extreme Values of Independent Stochastic Processes," *J. Appl. Probab.*, 14, 732–739.

Davison, A. C., Padoan, S. A., and Ribatet, M. (2012), "Statistical modeling of spatial extremes," *Stat. Sci.*, 27, 161–186.

de Haan, L. (1984), "A spectral representation for max-stable processes," *Ann. Probab.*, 12, 1194–1204.

de Haan, L. and Ferreira, A. (2006), *Extreme Value Theory: An Introduction*, Berlin: Springer.

Dieker, A. B. and Mikosch, T. (2014), "Exact simulation of Brown-Resnick random fields," Available from `http://arxiv.org/abs/1406.5624`.

Dombry, C. and Éyi-Minko, F. (2012), "Strong mixing properties of max-infinitely divisible random fields," *Stochastic Process. Appl.*, 122, 3790–3811.

— (2013), "Regular conditional distributions of continuous max-infinitely divisible random fields," *Electron. J. Probab*, 18, 1–21.

Engelke, S., Kabluchko, Z., and Schlather, M. (2011), "An equivalent representation of the Brown-Resnick process," *Statist. Probab. Lett.*, 81, 1150–1154.

Engelke, S., Malinowski, A., Oesting, M., and Schlather, M. (2014), "Statistical inference for max-stable processes by conditioning on extreme events," *Adv. Appl. Probab.*, 46, 478–495.

Giné, E., Hahn, M. G., and Vatan, P. (1990), "Max-infinitely divisible and max-stable sample continuous processes," *Probab. Th. Rel. Fields*, 87, 139–165.

Kabluchko, Z., Schlather, M., and de Haan, L. (2009), "Stationary Max-Stable Fields Associated to Negative Definite Functions," *Ann. Probab.*, 37, 2042–2065.

Oesting, M., Kabluchko, Z., and Schlather, M. (2012), "Simulation of Brown-Resnick Processes," *Extremes*, 15, 89–107.

Oesting, M., Schlather, M., and Zhou, C. (2013), "On the Normalized Spectral Representation of Max-Stable Processes on a Compact Set," Available from `http://arxiv.org/abs/1310.1813v1`.

Opitz, T. (2013), "Extremal t processes: Elliptical domain of attraction and a spectral representation," *J. Multivar. Anal.*, 122, 409–413.

Penrose, M. D. (1992), "Semi-min-stable processes," *Ann. Probab.*, 20, 1450–1463.

Resnick, S. I. and Roy, R. (1991), "Random usc functions, max-stable processes and continuous choice," *Ann. Appl. Probab.*, 1, 267–292.

Ribatet, M., Singleton, R., and team, R. C. (2013), *SpatialExtremes: Modelling Spatial Extremes*, R package version 2.0-0.

Schlather, M. (2002), "Models for stationary max-stable random fields," *Extremes*, 5, 33–44.

Schlather, M., Malinowski, A., Oesting, M., Boecker, D., Strokorb, K., Engelke, S., Martini, J., Menck, P., Gross, S., Burmeister, K., Manitz, J., Singleton, R., Pfaff, B., and Team, R. C. (2014), *RandomFields: Simulation and Analysis of Random Fields*, R package version 3.0.10.

Schlather, M. and Tawn, J. A. (2003), "A dependence measure for multivariate and spatial extreme values: Properties and inference," *Biometrika*, 90, 139–156.

Smith, R. L. (1990), "Max-stable processes and spatial extremes," Unpublished manuscript.

Stoev, S. A. and Taqqu, M. S. (2005), "Extremal stochastic integrals: a parallel between max-stable processes and α-stable processes," *Extremes*, 8, 237–266.

Stoyan, D., Kendall, W., and Mecke, J. (1995), *Stochastic Geometry and its Applications*, Chichester: John Wiley & Sons, 2nd ed.

Index